Long-Term Behavior of SIBOR® – an Oxidation Protection System for Mo and its Alloys

J. Januschewsky*, S. Engelhardt**, I. Dreiling*, M. Kathrein*, L.S. Sigl*

* PLANSEE SE, 6600 Reutte, Austria
** Technical University Dresden, 01062 Dresden, Germany

Abstract

A substantial disadvantage of molybdenum is its instability in the presence of oxygen, which is due to the formation of volatile oxides. To overcome this drawback, a silicon and boron based oxidation protection coating (trade name SIBOR®) was developed in the past years. This paper examines the long-term behavior of SIBOR® in air at temperatures of 1450°C and 1650°C and annealing times of up to 500 h by metallography in combination with chemical (EDS, WDS) and crystallographic (EBSD) spectroscopy.

After atmospheric plasma spraying of a Si-B-C mixture and subsequent short time annealing in hydrogen, a transient silicide/boride layer system develops which comprises a thick layer of $MoSi_2$ at the surface followed by thinner films of Mo_5Si_3, MoB_2 and MoB respectively. Upon further annealing, Mo-diffusion from the Mo-substrate transforms the initial silicides and borides eventually into thermodynamically stable Mo-rich compounds, i.e. Mo_3Si, and the ternary T_2-phase Mo_5SiB_2.

During exposure to air, a protective and a self-healing silica layer develops at the surface. The phase transformation in the silicide/boride layer system below the surface occurs concurrently with the oxidation, but is basically unaffected by the presence of oxygen. The stability and the self-healing capability of the SiO_2 layer are controlled by the composition of the Mo-silicide phase adjacent to it. While the silica layer is stable in the presence of $MoSi_2$, where it supplies excellent oxidation protection as indicated by a parabolic thickness-growth behavior, the transformation of $MoSi_2$ into Mo_5Si_3 and later into Mo_3Si reduces the stability of the silica layer drastically. Thus, the oxidation shielding of SIBOR® relies on the presence of a continuous $MoSi_2$ layer beneath the protecting silica layer, and hence depends largely on the transformation kinetics of the initial silicide/boride layer system.

Keywords

SIBOR®, molybdenum, oxidation protection, coating, molybdenum silicides, molybdenum borides, silica

Introduction

In addition to the demand for materials with low thermal expansion, high thermal conductivity and good mechanical properties at high temperatures (such as strength and creep resistance), sufficient resistance to corrosion and oxidation is mandatory in many industrial applications. Mo has excellent mechanical and physical properties, yet suffers from poor oxidation resistance at temperatures above 400°C. An effective method to protect it against oxidation are Si-based coatings. For more than 10 years a Si- and B-based oxidation protection coating on Mo, and recently also on Mo-ZrO_2, has been used commercially under the brand name SIBOR®. SIBOR® was developed in particular for the demands of the glass industry [1-3].

Over the last years, the Mo-Si-B system has been studied intensively. Different Mo-silicide alloys [7,8], Mo-Si-B-alloys [9-15] and silicide coatings with [16] and without boron [17] were investigated. The aim of this study is to examine the long-term behavior of SIBOR® coatings at typical operation temperatures in air, i.e. at 1450°C and 1650°C. In order to elucidate the life limiting processes, the reactions of SIBOR® with air and with the Mo substrate will be analyzed and discussed.

Experimental

Fully dense molybdenum rods (diameter 12 mm) were sand blasted and then coated with a 200 µm Si-B-C layer by APS (starting composition 10 wt.% B, 2 wt.% C, remainder Si). After annealing *in hydrogen* for 45 mins. at 1450°C, a silicide/boride layer system develops, i.e. a surface layer of $MoSi_2$ is followed by thin films of Mo_5Si_3, MoB and Mo_2B respectively (cf. Fig. 1, details can be found elsewhere [4-6]). Subsequently, a second annealing was performed *in air* in a muffle furnace for 10, 100 and 500 hours respectively at 1450°C and 1650°C at a heat up rate of 10 K/min.

For each time and temperature, an extra sample was prepared and analyzed. The weight of every sample was measured before and after the exposure to air with a Mettler Toledo XP 204S analysis balance. The phases were identified by a combination of EDS/WDS and EBSD measurements according to the procedure described in [4]. Details of the metallographic preparation and of the SEM analysis are given elsewhere [4,5].

Results

A scanning electron micrograph and an EBSD phase mapping of the SIBOR® coating system after the initial hydrogen treatment are shown in Fig. 1. The sequence of layers after the hydrogen anneal is typical for the SIBOR® system: a thick $MoSi_2$ layer at the surface (thickness ≈ 90-120 µm) is followed by a thin Mo_5Si_3 film (thickness ≈ 6 µm) and two even thinner boride films (MoB and Mo_2B, thickness < 5 µm), which are located above the Mo substrate [cf. 4-6]. A band of small pores at a depth of ≈ 50-70 µm is also evident in Fig. 1a.

After a 10 h exposure to air at 1450°C, a partially crystalline silica layer has formed *at the surface* (Fig. 2). The SiO_2 layer is continuous, yet varies considerably in thickness (Fig. 2a). It contains traces of boron (approx. 1-3 wt.% as assessed by WDS) independent of the applied exposure time or temperature. The determination of the B content is subject to some uncertainty due to the rough surface structure of the silica, since deviations from planar surfaces do affect the precision of WDS. *Inside* the SIBOR® layer, the

Mo_5Si_3 film has grown significantly at the expense of $MoSi_2$, and the MoB phase has disappeared, i.e. Mo_2B remains the only B-containing phase after an annealing time of 10 h. The band of pores at a depth of ≈ 50-70 µm is still present, yet the pore size has decreased.

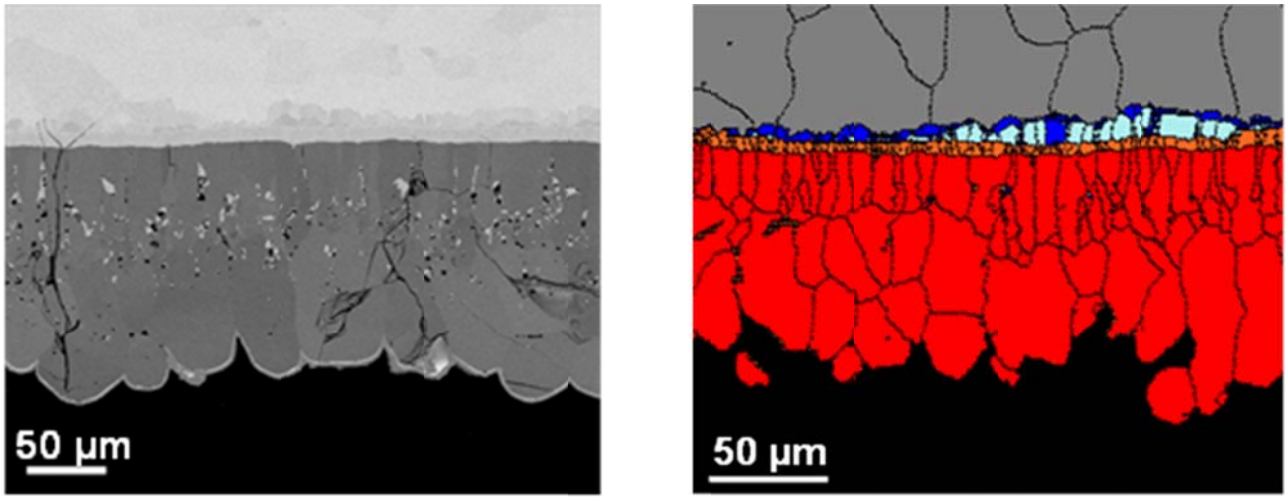

(a) (b)

Figure 1: (a) SEM-BSE image of a cross-section through a SIBOR®-coated Mo sample after hydrogen annealing. (b) EDS-EBSD phase assignment of (a) including grain boundaries (local differences in orientation >5°). Color code: red-$MoSi_2$; orange-Mo_5Si_3; light-blue-MoB; blue-Mo_2B; grey-Mo; black: grain boundaries.

Annealing for 100 h at 1450°C increases the thickness of the silica layer as expected (Fig. 3a). The growth rate follows a parabolic behavior as shown in Fig. 5. Most important, the thickness of the Mo_5Si_3 layer has further increased, again at the expense of $MoSi_2$ (Fig. 3b). Further, Mo_2B has precipitated at the grain boundaries of the Mo substrate and, for the first time, the ternary T_2-phase Mo_5SiB_2 is detected in the vicinity of Mo_5Si_3 and Mo_2B.

After 500 h at 1450°C, the $MoSi_2$ phase has completely disappeared and Mo_5Si_3 has become the dominating phase in the system (Fig. 4). It should be noted that the silica layer at the surface is now bounded by Mo_5Si_3 rather than by $MoSi_2$. Furthermore, Mo_2B has almost disappeared while the T_2-phase (Mo_5SiB_2), forming a band-like structure which is embedded into the Mo_5Si_3 layer, has become the major B-containing phase. Noteworthy, the T_2-phase coexists with virtually all phases in the Mo-rich corner of the Mo-Si-B system (Fig. 7). Fig. 4 also shows a high level of porosity at the outer zone of the Mo_5Si_3 layer. Finally, Mo_3Si has formed at both sides of the Mo_5Si_3 layer, i.e. predominantly at the interface between Mo_5Si_3/Mo and to a small extent at the Mo_5Si_3/SiO_2 interface.

Fig. 5 shows the mass change of SIBOR® samples after different exposure times in air at 1450°C. All samples up to 250 hours exposure time have gained mass, whereas a significant mass *loss* of 68 mg/cm² is observed after 500 h in air. The growth rate of the film thickness up to 250 h follows a parabolic law according to

$$\left(\frac{\Delta m}{A}\right)^2 = k_m\, t \qquad (1)$$

where Δm is the mass gain of the sample due to the silica film formation, A is the specimen surface area and k_m is the mass related parabolic growth rate constant. k_m was determined from equation (1) by least square fitting to be $4 \cdot 10^{-10}$ kg²/m⁴s.

(a) (b)

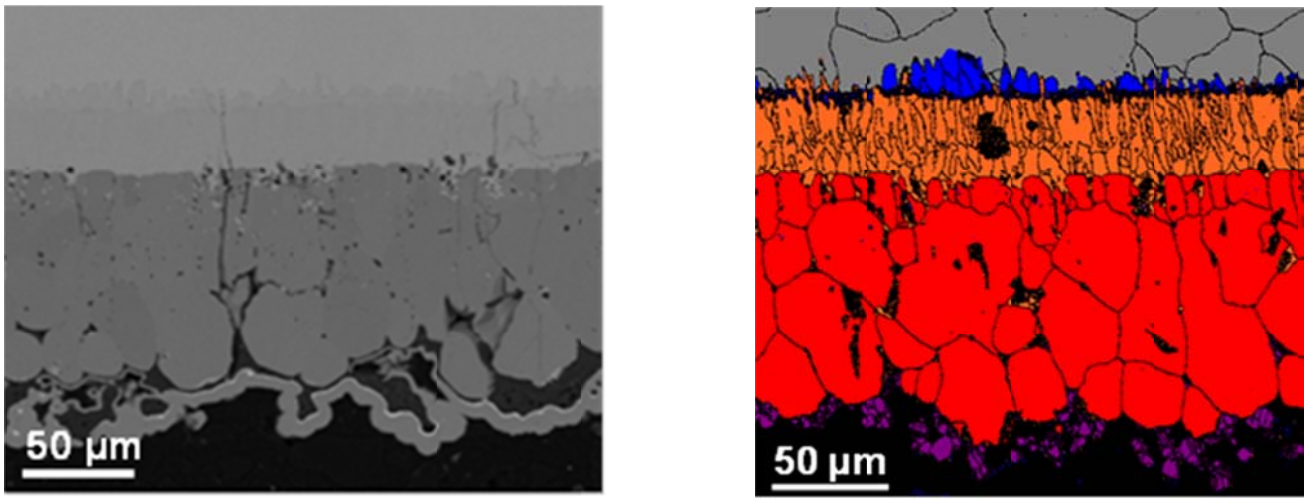

Figure 2: 10 h at 1450°C in air.

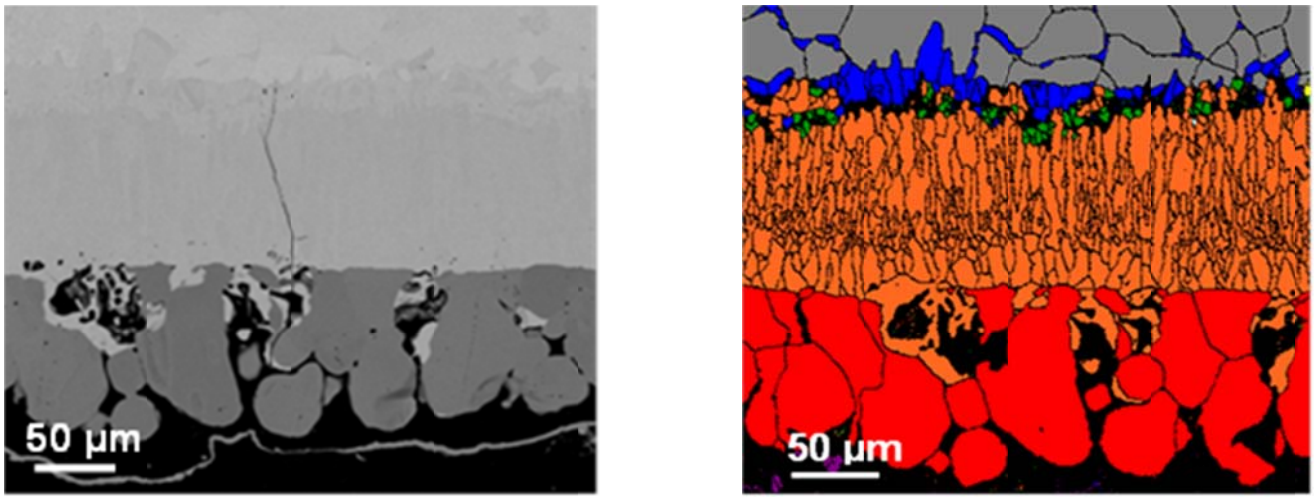

Figure 3: 100 h at 1450°C in air.

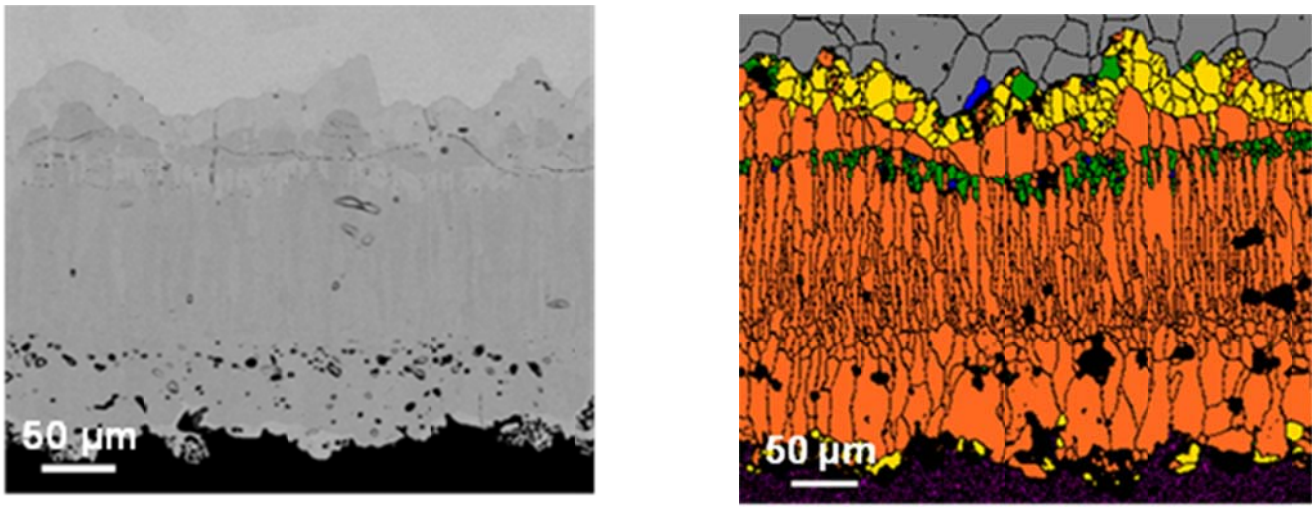

Figure 4: 500 h at 1450°C in air.

Figures 2-4: (a) SEM-BSE images of a cross section through a SIBOR®-coated Mo sample.
(b) EDS-EBSD phase assignment with grain boundaries (local orientation difference >5°). Color code: red-$MoSi_2$; orange-Mo_5Si_3; yellow-Mo_3Si, blue-Mo_2B; green-Mo_5SiB_2; violet-SiO_2 ; grey-Mo; black: grain boundaries.

This number is in good agreement with the value of 10^{-10} kg²/m⁴s, which Sharif recently reported for the oxidation of pure $MoSi_2$ at 1400°C [18]. The mass *loss* after 500 h indicates the failure of the oxidation protection system, which is also evident from visual inspection. It coincides with the full replacement of the $MoSi_2$- by the Mo_5Si_3-layer.

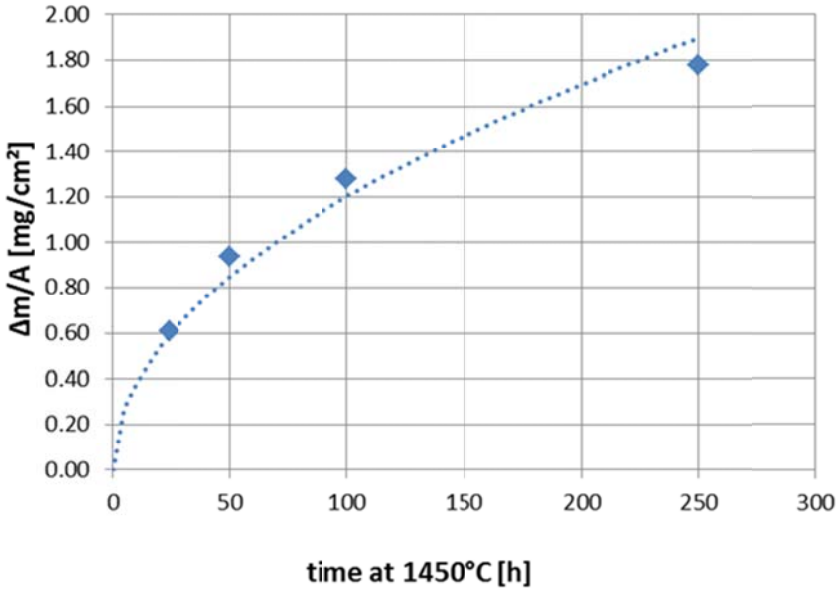

Figure 5: Mass gain of SIBOR® samples at 1450°C in air.

At an annealing temperature of 1650 °C, the phase evolution in the SIBOR® coating is basically similar to the situation at 1450 °C, yet much faster. After 10 h at 1650°C the Mo_5Si_3 layer has grown nearly as much as after 100 h at 1450°C (Fig. 5), i.e. the thickness of the Mo_5Si_3 layer is comparable to the situation after 100 h at 1450°C (cf. Figs. 3 and 5). The Mo_2B phase has disappeared almost completely, and Mo_5SiB_2 can already be found. Likewise, the first Mo_3Si precipitates have emerged between Mo_5Si_3 and Mo, a feature that is observed at 1450°C only after > 100 h annealing.

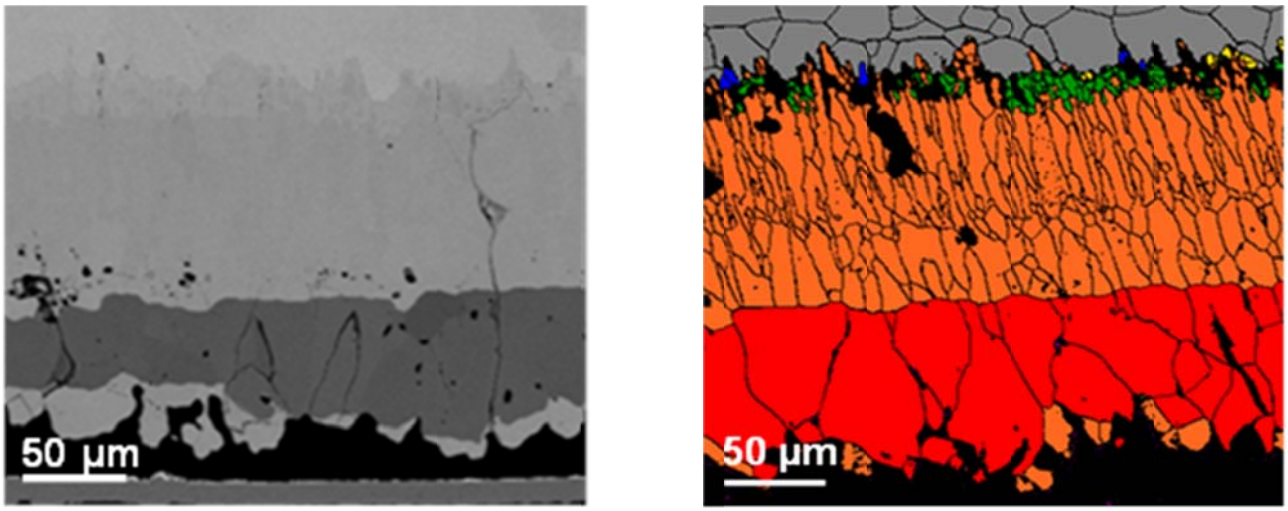

(a) (b)

Figure 6: (a) SEM-BSE images of a cross section through a SIBOR®-coated Mo sample after 10 h at 1650 °C in air. (b) EDS-EBSD phase assignment with grain boundaries (local orientation difference >5°). Color code: red-$MoSi_2$; orange-Mo_5Si_3; yellow-Mo_3Si, blue-Mo_2B; green-Mo_5SiB_2; violet-SiO_2 ; grey-Mo; black: grain boundaries.

Discussion

The compositional evolution of the phases in the diffusion couple Mo/(Si-B), which have been exposed to *short* annealing in hydrogen, was elaborated earlier by Traxler et al. and Kriegel et al. [4,6]. They showed that single-phase layers of Si- and B-compounds develop above the Mo-substrate, with the sequence Mo, Mo_2B, MoB, Mo_5Si_3 and $MoSi_2$, respectively. Additionally, fine Kirkendall pores were observed in the $MoSi_2$ layer, which were attributed to the fast diffusion of boron into the Mo substrate. The layered phases observed in Fig. 1 are in ample agreement with those results.

Most important, the present study reveals that the phase arrangement after short term hydrogen annealing is *unstable* in the presence of excess Mo, as expected from the Mo-Si-B phase diagram shown in Fig. 7. During long time, high-temperature annealing of the phase-layers on top of the Mo substrate, the transient phase arrangement of Mo_2B, MoB, Mo_5Si_3 and $MoSi_2$ transforms into stable Mo-compounds as demanded by the Mo-Si-B phase diagram (Fig. 7).

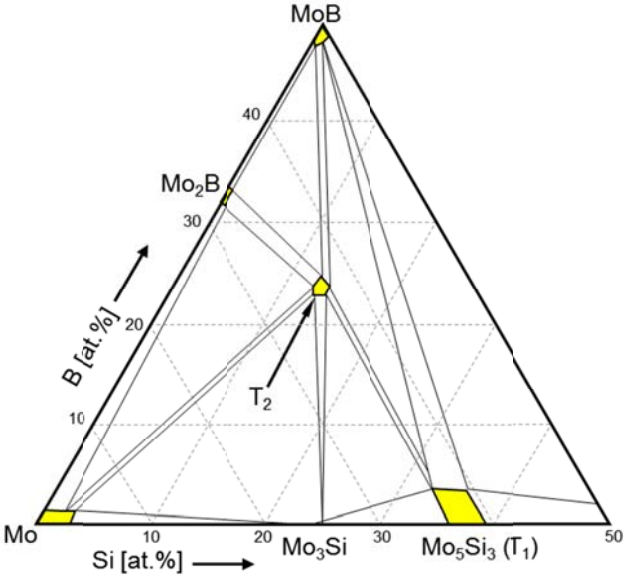

Figure 7: Isothermal section through the Mo-rich corner of the Mo-Si-B phase diagram at 1450°C.

(i) Equilibration of the Si-phases and B-phases

In fact, our observations show that the $MoSi_2$ layer vanishes continuously in favor of Mo_5Si_3 and finally of $MoSi_3$ respectively. Figs. 2 and 3 illustrate the growth of the Mo_5Si_3 layer thickness at the expense of the $MoSi_2$ layer as compared to the preliminary phases in the H_2-annealed SIBOR® coating (Fig. 1).These observations can be readily understood as an evolution of the diffusion couples $Mo/MoSi_2$ and Mo/Mo_5Si_3 into the finally stable couple Mo/Mo_3Si. The $Mo/MoSi_2$ and Mo/Mo_5Si_3 diffusion couples enforce the consecutive formation of Mo_5Si_3 and Mo_3Si respectively, i.e. $MoSi_2$ is eventually transformed via Mo_5Si_3 into Mo_3Si. The growth of Mo_3Si has been reported to be slower than the growth of Mo_5Si_3 [8]. Consequently, only after long annealing times (Fig. 4b) and/or higher temperatures (Fig. 6b) can the formation of Mo_3Si be observed.

A similar equilibration process happens to the Mo-borides, where the stable ternary T_2-phase (Mo_5SiB_2) develops at the expense of the binary Mo-borides MoB and Mo_2B. The initial MoB transforms completely into the more stable Mo_2B within 10 h at 1450°C (Fig. 2b), and after 100 h the precipitation of Mo_2B is observed at the Mo-grain boundaries (Fig. 3b). In summary, again, a transformation process into a ther-

modynamically more stable phase arrangement takes place, which ultimately contains Mo_5SiB_2, Mo and Mo_3Si only. Notably, despite the fact that the intermediate Mo_2B is chemically compatible with Mo, the excess of Si over B, drives the system into the Mo-Mo_5SiB_2-Mo_3Si phase triangle (Fig. 7) which does not permit the presence of Mo_2B.

(ii) Formation and stability of the silica layer

Superimposed on the equilibration reactions in the Mo-Si-B system are surface reactions due to the presence of oxygen in the atmosphere. Firstly, oxygen generates a silica layer at the surface of SIBOR® coatings by reacting with $MoSi_2$. On the other hand, it should be recalled, that the equilibration reactions in the SIBOR® system discussed above are continuing, despite the presence of oxygen at the surface. The reaction of $MoSi_2$ with oxygen on the surface is most likely a full oxidation according to the reaction

$$MoSi_2 + \frac{7}{2}O_2 \rightarrow MoO_3 + 2\,SiO_2 \qquad (2)$$

Since MoO_3 is highly volatile above 600°C, it is expected to evaporate readily. From the parabolic mass gain shown in Fig. 5 we conclude, that a dense SiO_2 layer forms on the surface and that the progress of oxidation is controlled by the diffusion of oxygen through the silica layer. This process continues until Mo_5Si_3 has fully replaced $MoSi_2$. Then the oxygen will react with Mo_5Si_3 according to

$$Mo_5Si_3 + \frac{21}{2}O_2 \rightarrow 5\,MoO_3 + 3\,SiO_2 \qquad (3)$$

Compared to reaction (2), reaction (3) generates more than 3 times as much volatile MoO_3 per mole of SiO_2. We believe, that the much increased vapor pressure of the extra MoO_3 destabilizes and damages the silica layer, such that the oxidation protection gets lost. This hypothesis is compatible with the observation that the significant mass loss after 500 h at 1450 °C happens only after the Mo_5Si_3 has fully replaced the $MoSi_2$. Of course, the properties of the silica layer are also important in this process, in particular the thermal expansion mismatch, its crystallinity and viscosity, which depend amongst others on temperature and the amount of B. Nevertheless, with the self-healing ability being suppressed by the excess MoO_3, any defect within the protective SiO_2 layer will readily lead to a failure of the protective system.

Conclusions

SIBOR® coated Mo samples were systematically heat-treated in air at 1450°C and 1650°C for up to 500 hours. As long as $MoSi_2$ constitutes the layer below the silica, the mass gain obeys a parabolic law, which indicates the diffusion controlled growth of a dense and protective SiO_2 layer. Superimposed on the surface oxidation is the evolution of thermodynamically stable Si- and B-compounds in the layers below the protective silica film. Essentially, the transformation of the highly oxidation resistant $MoSi_2$ into Mo_5Si_3 limits the oxidation protection of the SIBOR® system at high temperatures. At 1650°C virtually identical, yet much accelerated process mechanisms are observed. The consumption of the oxidation resistant $MoSi_2$ phase being much faster, reduces the life time of SIBOR® at 1650 °C significantly. Thus, the oxidation shielding of SIBOR® relies on the presence of a continuous $MoSi_2$ layer beneath the protecting silica layer, and hence depends essentially on the transformation kinetics of the initial silicide/boride layer system.

References

1. H.P. Martinz, J. Matej and G. Leichtfried, *Proceedings 15th Plansee Seminar*, Reutte, pp. 217-228, (2001)
2. H.P. Martinz, B. Nigg, J. Matej, M. Sulik and H. Larcher, *Adv. Mater. Res.* **39-40,** 613-618, (2008)
3. H.P. Martinz, B. Nigg, J. Matej, M. Sulik, H. Larcher and A. Hoffmann, *Int. J. Refract. Met. Hard Mater.* **24** [4], 283-291, (2006)
4. H. Traxler, R. Jörg, M. Zabernig and L.S. Sigl, *Pract. Metallogr*. **48** [9], 428-441, (2011)
5. I. Dreiling, M. Sulik, J. Januschewsky and L.S. Sigl, *46. MetallographieTagung, 19.-21.Sept., Rostock,* (2012)
6. M.J. Kriegel, W. Foerster, D. Chmelik, O. Fabrichnaya, J. Januschewsky, M. Kathrein, L.S. Sigl and D. Rafaja, *this conference,* (2013)
7. K. Bundschuh and M. Schütze, *Materials and Corrosion* **52**, 268-282, (2001)
8. J.-K. Yoon, J.-Y. Byun, G.-H. Kim, J.-S. Kim, C.-S. Choi, *Thin Solid Films* **405**, 170-178 (2002)
9. M.G. Mendiratta, T.A. Parthasarathy and D.M. Dimiduk, *Intermetallics* **10** [3], 225-232, (2002)
10. R. Sakidja, J.S. Park, J. Hamann and J H. Perepezko, *Script. Mat*. **53**, 723-728, (2005)
11. S. Burk, B. Gorr, V. B. Trinidade, U. Krupp and H.-J. Christ, *Corr. Engineering, Science and Technology* **44** [3], 168-175, (2009)
12. S. Burk, B. Gorr and H.-J. Christ, *Acta Mat*. **58**, 6154-6165, (2010)
13. M.K. Meyer and M. Akinc, *J. Am. Ceram. Soc*. **79** [4], 938-944, (1996)
14. C. Nunes, R. Sakidja, Z. Dong and J.H. Perepezko, *Intermetallics* **8**, 327-337, (2000)
15. R. Sakidja and J.H. Perepezko, *J. Nucl. Mat*. **366**, 407-416, (2007)
16. J.H. Perepezko, F. Rioult and R. Sakidja, *Mat. Sci. For*. **595-598**, 1065-1074, (2008)
17. M. Zafir Alam, B. Venkataraman, B. Sarma and D.D. Das, *J. Alloys and Compounds* **487**, 335-340, (2009)
18. A.A. Sharif, *J. Mater. Sci.* **45**, 865-870, (2010)